

Construction of optimal 3-node plate bending triangles by templates

C. A. Felippa, C. Militello

1

Abstract A finite element template is a parametrized algebraic form that reduces to specific finite elements by setting numerical values to the free parameters. The present study concerns Kirchhoff Plate-Bending Triangles (KPT) with 3 nodes and 9 degrees of freedom. A 37-parameter template is constructed using the Assumed Natural Deviatoric Strain (ANDES). Specialization of this template includes well known elements such as DKT and HCT. The question addressed here is: can these parameters be selected to produce high performance elements? The study is carried out by staged application of constraints on the free parameters. The first stage produces element families satisfying invariance and aspect ratio insensitivity conditions. Application of energy balance constraints produces specific elements. The performance of such elements in benchmark tests is presently under study.

1

Introduction

This is a revised version of a paper (Felippa and Militello, 1998) contributed to the IV World Congress on Computational Mechanics. That paper dealt with the construction of high-performance (HP) 3-node triangular finite elements for thin plate bending using the template approach. The main revision has been a more systematic investigation of template constraints, and in particular invariant conditions. This in turn has clarified how existing elements such as DKT and AQR fit into element families. The ordering of template coefficients has been changed to better fit those conditions.

C.A. Felippa (✉)
Department of Aerospace Engineering Sciences
and Center for Aerospace Structures,
University of Colorado at Boulder,
Boulder, Colorado 80309-0429,
USA

C. Militello
Departamento de Física Fundamental y Experimental
Universidad de la Laguna,
La Laguna, Tenerife,
Spain

Preparation of the present paper has been supported by the National Science Foundation under Grant ECS-9725504, and by Sandia National Laboratories under the Advanced Strategic Computational Initiative (ASCI) Contract AS-9991.

2

High performance finite elements

An important objective of present FEM research is the construction of high performance (HP) finite elements. These have been defined (Felippa and Militello, 1989) as *simple elements that deliver engineering accuracy with arbitrary coarse meshes*. This definition requires further clarification.

Simple means the simplest geometry and freedom configuration that fits the problem and target accuracy, consistent with human and computer resources. This can be summed up in one FEM modeling rule: *use the simplest element that will do the job*.

Engineering accuracy is that generally expected in most FEM applications in Aerospace, Civil and Mechanical Engineering. Typically this is 1% in displacements and 10% in strains, stresses and derived quantities. Some applications, notably in Aerospace, may require higher precision in quantities such as natural frequencies, shape tolerances, or in long-time dynamic simulations.

Coarse mesh is one that suffices to capture the important physics in terms of geometry, material and load properties. It does not imply few elements. For example, a coarse mesh for an aircraft undergoing combat maneuvers may require several million elements. For simple benchmark problems such as a uniformly loaded square plate, a mesh of 4 or 16 elements may be classified as coarse.

Finally, the term *arbitrary mesh* implies *low sensitivity* of the solution to element aspect ratio, skewness, distortion and mesh directionality effects. This attribute is becoming important as push-button mesh generators gain importance, because automatically generated unstructured meshes can be of low quality compared to those produced by an experienced analyst.

For practical reasons we are interested only in the construction of HP elements with *displacement* nodal degrees of freedom. Such elements are characterized by their stiffness equations, and thus can be plugged into any standard finite element program.

3

From PVPs to templates

The approach to HP elements taken by the first author started in 1984 from collaborative work with Bergan in Free Formulation (FF) high performance elements. The results of this collaboration were a membrane triangle with drilling freedoms (Bergan and Felippa, 1965) and a plate bending triangle (Felippa and Bergan, 1985). It continued with exploratory work using the Assumed Natural Strain

(ANS) method of Park and Stanley (1986). Eventually FF and ANS coalesced in a variant of ANS called Assumed Natural Deviatoric Strain, or ANDES. Elements based on ANDES are described by Militello and Felippa (1991).

This unification work led naturally to a formulation of elasticity functionals containing free parameters. These were called *parametrized variational principles*, or PVPs in short. Setting the parameters to specific numerical values produced the classical functionals of elasticity such as Total Potential Energy, Hellinger-Reissner and Hu-Washizu. For linear elasticity, 3 free parameters in a 3-field functional with independently varied displacements, strains and stresses are sufficient to embed all classical functionals. The Euler-Lagrange equations of a PVP do reproduce the field equations but with different weights. Two survey articles: (Felippa, 1994) and (Felippa, 1996) contain references to the development of PVPs and the original papers of the 1980s. These may be consulted for practical and historic details. An extension to dynamic modeling has recently been published (Brito Castro et al., 1997).

One result from the PVP formulation is that, upon FEM discretization, free parameters appear at the element level. One thus naturally obtains *families* of elements. Setting the free parameters to numerical values produces specific elements. Although the PVP Euler-Lagrange equations are the same excepts for weights, the discrete solution produced by different elements are not. Thus an obvious question arises: which free parameters produce the best elements? It turns out that there is no clear answer to the question, because the best set of parameters depends on the element geometry. Hence the equivalent question: which is the best variational principle? makes no sense.

The PVP formulation led, however, to an unexpected discovery. The configuration of elements constructed according to PVPs and the usual assumptions on displacements, stresses and strains was observed to follow specific algebraic rules. *Such configurations could be parametrized directly without going through the source PVP.* This observation led to a general formulation of finite elements as *templates*.

4 Finite element templates

A finite element template, or simply *template*, is an algebraic form that represents element-level stiffness equations, and which fulfills the following conditions:

(C) Consistency: the Individual Element Test (IET) form of the patch test, introduced by Bergan and Hansen (1975), is passed for any element geometry.

(S) Stability: the element stiffness matrix satisfies correct rank and nonnegativity conditions.

(P) Parametrization: the element stiffness equations contain free parameters.

(I) Invariance: the element equations are observer invariant. In particular, they are independent of node numbering and choice of reference systems.

The first two conditions: (C) and (S), are imposed to ensure convergence. Property (P) permits optimization as well as tuning elements to specific needs. Property (I) helps predictability and benchmark testing.

Setting the free parameters to numeric values yields specific element instances.

4.1 The fundamental decomposition

A stiffness matrix derived through the template approach has the fundamental decomposition

$$\mathbf{K} = \mathbf{K}_b(\alpha_i) + \mathbf{K}_h(\beta_j) \quad (1)$$

Here \mathbf{K}_b and \mathbf{K}_h are the basic and higher-order stiffness matrices, respectively. The basic stiffness matrix \mathbf{K}_b is constructed for *consistency* and *mixability*, whereas the higher order stiffness \mathbf{K}_h is constructed for *stability* (meaning rank sufficiency and nonnegativity) and *accuracy*. As further discussed below, the higher order stiffness \mathbf{K}_h must be orthogonal to all rigid-body and constant-strain (curvature) modes.

In general both matrices contain free parameters. The number of parameters α_i in the basic stiffness is typically small for simple elements. For example, in the 3-node KPT elements considered here there is only one basic parameter, called α . This number must be the same for all elements in a mesh to insure satisfaction of the IET (Bergan and Felippa, 1985).

On the other hand, the number of higher order parameters β_j can be in principle *infinite* if certain components of \mathbf{K}_h can be represented as polynomial series of element geometrical invariants. In practice, however, such series are truncated, leading to a finite number of β_j parameters. Although the β_j may vary from element to element without impairing convergence, often the same parameters are retained for all elements.

4.2 Constructing the component stiffness matrices

The basic stiffness that satisfies condition (C) is the same for any formulation. It is simply a constant stress hybrid element (Bergan and Nygård, 1984; Bergan and Felippa, 1985). For a specific element and freedom configuration, \mathbf{K}_b can be constructed once and for all.

The formulation of the higher order stiffness \mathbf{K}_h is not so clear-cut, as can be expected because of the larger number of free parameters. It can be done by a variety of techniques, which are summarized in a recent article (Felippa, Haugen and Militello, 1995). Of these, one has proven exceedingly useful for the construction of templates: the ANDES formulation. ANDES stands for Assumed Natural DEviatoric Strains. It is based on assuming natural strains for the high order stiffness. For plate bending (as well as beams and shells) natural curvatures take the place of strains.

Second in usefulness is the Assumed Natural DEviatoric STRESSes or ANDESTRESS formulation, which for bending elements reduces to assuming deviatoric moments. This technique, which leads to stiffness templates that contain inverses of natural flexibilities, is not considered here.

4.3 Basic stiffness properties

The following properties of the template stiffness equations are collected here for further use. They are discussed

in more detail in the article by Felippa, Haugen and Militelto (1995). Consider a test displacement field, which for the KPT would be a continuous transverse displacement mode $w(x, y)$. [In practical computations this will be a polynomial in x and y .] Evaluate this at the nodes to form the element node displacements \mathbf{u} . These can be decomposed into

$$\mathbf{u} = \mathbf{u}_b + \mathbf{u}_h = \mathbf{u}_r + \mathbf{u}_c + \mathbf{u}_h, \quad (2)$$

where \mathbf{u}_r , \mathbf{u}_c and \mathbf{u}_h are rigid body, constant strain and higher order components, respectively, of \mathbf{u} . The first two are collectively identified as the *basic* component \mathbf{u}_b . The matrices (1) must satisfy the stiffness orthogonality conditions

$$\mathbf{K}_b \mathbf{u}_r = \mathbf{0}, \quad \mathbf{K}_h \mathbf{u}_r = \mathbf{0}, \quad \mathbf{K}_h \mathbf{u}_c = \mathbf{0} \quad (3)$$

while \mathbf{K}_b represents exactly the response to \mathbf{u}_c .

The strain energy taken up by the element under application of \mathbf{u} is $U = \frac{1}{2} \mathbf{u}^T \mathbf{K} \mathbf{u}$. Decomposing \mathbf{K} and \mathbf{u} as per (1) and (2), respectively, and enforcing (3) yields

$$U = \frac{1}{2} (\mathbf{u}_b + \mathbf{u}_h)^T \mathbf{K}_b (\mathbf{u}_b + \mathbf{u}_h) + \frac{1}{2} \mathbf{u}_h^T \mathbf{K}_h \mathbf{u}_h = U_b + U_h \quad (4)$$

U_b and U_h are called the basic and higher order energy, respectively. Let U_{ex} be the exact energy taken up by the element as a continuum body subjected to the test displacement field. The element energy ratios are defined as

$$\rho = \frac{U}{U_{ex}} = \rho_b + \rho_h, \quad \rho_b = \frac{U_b}{U_{ex}}, \quad \rho_h = \frac{U_h}{U_{ex}}. \quad (5)$$

Here ρ_b and ρ_h are called the basic and higher order energy ratios, respectively. If $\mathbf{u}_h = \mathbf{0}$, $\rho = \rho_b = 1$ because the element must respond exactly to any basic mode by construction. For a general displacement mode in which \mathbf{u}_h does not vanish, ρ_b is a function of the α_i whereas ρ_h is a function of the β_j .

4.4

Constructing optimal elements

By making a template sufficiently general all published finite elements for a specific configuration can be generated. This includes those derivable by orthodox techniques (for example, shape functions) and those that are not. Furthermore, an infinite number of new elements arise. The same question previously posed for PVPs arises: Can one select the free parameters to produce an optimal element?

The answer is not yet known for general elements. The main unresolved difficulty is: which optimality conditions must be imposed at the local (element) level? While some of them are obvious, notably those leading to observer invariance, most of the others are not. The problem is that *a detailed connection between local and global optimality is not fully resolved by conventional FEM error analysis*. Such analysis can only provide convergence rates expressed as Ch^m in some error norm, where h is a characteristic mesh dimension and m is usually the same for all template instances. The key to high performance is the coefficient C , but this is problem dependent. Consequently, verification benchmarks are still inevitable.

Because conventional error analysis is of limited or no value, most of the template optimization constraints discussed later are heuristic. But even if the local-to-global connection were fully resolved, a second technical difficulty arises: the actual construction and optimization of templates poses formidable problems in symbolic matrix manipulation, because one has to carry along arbitrary geometries, materials and free parameters. Until recently those manipulations were beyond the scope of computer algebra systems (CAS) for all but the simplest elements. As personal computers and workstations gain in CPU speed and storage, it is gradually becoming possible to process two-dimensional elements for plane stress and plate bending. Most three-dimensional and curved-shell elements, however, still lie beyond the power of present systems.

Practitioners of optimization are familiar with the dangers of excessive perfection. A system tuned to operate optimally for a narrow set of conditions often degrades rapidly under deviation from such conditions. We will see that a similar difficulty exists in the construction of optimal plate elements, and that expectations of an “element for all seasons” must be tempered.

5

Templates for 3-node KPT elements

The application of the template approach is rendered specific by studying a particular configuration: a 3-corner-node flat triangular element to model bending of Kirchhoff (thin) plates. The element has the conventional 3 degrees of freedom: one transverse displacement and 2 rotations at each corner. For brevity this will be referred to as a Kirchhoff Plate Triangle, or KPT, in the sequel. The complete development of the template is given in the Appendix. Here we summarize only the important results necessary for the construction of HP elements.

5.1

Stiffness decomposition

For the KPT elements under study the configuration of the stiffness matrices in (1) can be shown in more detail. Assuming that the 3×3 moment-curvature plate constitutive matrix \mathbf{D} is constant over the triangle, we have

$$\mathbf{K}_b = \frac{1}{A} \mathbf{L} \mathbf{D} \mathbf{L}^T, \quad \mathbf{K}_h = \frac{A}{3} \left[\mathbf{B}_{\gamma 4}^T \mathbf{D}_{\gamma} \mathbf{B}_{\gamma 4} + \mathbf{B}_{\gamma 5}^T \mathbf{D}_{\gamma} \mathbf{B}_{\gamma 5} + \mathbf{B}_{\gamma 6}^T \mathbf{D}_{\gamma} \mathbf{B}_{\gamma 6} \right]. \quad (6)$$

Here A is the triangle area, \mathbf{L} is the 9×3 force lumping matrix that transforms a constant internal moment field to node forces, $\mathbf{B}_{\gamma m}$ are 3×9 matrices relating natural curvatures at triangle midpoints $m = 4, 5, 6$ to node displacements, and \mathbf{D}_{γ} is the plate constitutive matrix transformed to relate natural curvatures to natural moments. Parameter α appears in \mathbf{L} whereas parameters β_j appear in $\mathbf{B}_{\gamma m}$. Full expressions of these matrices are given in the Appendix.

5.2

The KPT-1-36 and KPT-1-9 templates

A useful KPT template is based on a 36-parameter representation of \mathbf{K}_h in which the series noted above retains up

to the *linear* terms in three triangle geometric invariants λ_1, λ_2 and λ_3 , defined in the Appendix. The template is said to be of *order one* in the λ s. It has a total of 37 free parameters: one α and 36 β s. Collectively the template is identified as KPT-1-36. Instances are displayed using the following tabular arrangement:

$$\begin{array}{c} \text{acronym } \alpha \ \beta_{10} \ \beta_{20} \ \beta_{30} \ \beta_{40} \ \beta_{50} \ \beta_{60} \ \beta_{70} \ \beta_{80} \ \beta_{90} \ / \beta_{sc} \\ \beta_{11} \ \beta_{21} \ \beta_{31} \ \beta_{41} \ \beta_{51} \ \beta_{61} \ \beta_{71} \ \beta_{81} \ \beta_{91} \\ \beta_{12} \ \beta_{22} \ \beta_{32} \ \beta_{42} \ \beta_{52} \ \beta_{62} \ \beta_{72} \ \beta_{82} \ \beta_{92} \\ \beta_{13} \ \beta_{23} \ \beta_{33} \ \beta_{43} \ \beta_{53} \ \beta_{63} \ \beta_{73} \ \beta_{83} \ \beta_{93} \end{array} \quad (7)$$

Here β_{sc} is a scaling factor by which all displayed β_{ij} must be divided; e.g. in the DKT element listed in Table 1 $\beta_{10} = -6/4 = -3/2$ and $\beta_{41} = 4/4 = 1$. If β_{sc} is omitted it is assumed to be one.

Setting the 37 parameters to numeric values yields, specific elements, identified by the acronym displayed on the left. Some instances that are interesting on account of practical or historical reasons are collected in Table 1. This represents a tiny subset of the number of published KPT elements, which probably ranges in the hundreds, and is admittedly biased in favor of elements developed by the authors. Table 2 identifies the acronyms of Table 1, correlated with original publications where appropriate.

An interesting subclass of (7) is that in which the bottom 3 rows vanish: $\beta_{11} = \beta_{12} = \dots = \beta_{93} = 0$. This 10-parameter template is said to be of *order zero* because the invariants λ_1, λ_2 and λ_3 do not appear in the higher order stiffness. It is identified as KPT-1-9. For brevity it will be written simply as

$$\text{acronym } \alpha \ \beta_{10} \ \beta_{20} \ \beta_{30} \ \beta_{40} \ \beta_{50} \ \beta_{60} \ \beta_{70} \ \beta_{80} \ \beta_{90} \ / \beta_{sc} \quad (8)$$

omitting the zero entries.

5.3

Element families

Specializations of (7) and (8) that still contain free parameters are called *element families*. In such a case the free parameters are usually written as arguments of the acronym. For example, Table 4 defines the ARI (Aspect Ratio Insensitive) family derived in Section 6. ARI has seven free parameters identified as $\alpha, \beta_{10}, \beta_{20}, \beta_{30}, \gamma_0, \gamma_1$ and γ_2 .

Consequently the template acronym is written

$$\text{ARI}(\alpha, \beta_{10}, \beta_{20}, \beta_{30}, \gamma_0, \gamma_1, \gamma_2).$$

A family whose only free parameter is α is called an α family. Its instances are called α variants. In some α families the β coefficients are fixed. For example in the AQR(α) and FF(α) families only α changes. Some practically important instances of those families are shown in Table 1. In other families, the β are functions of α . For example this happens in the BCIZ(α) family, two instances of which, obtained by setting $\alpha = 0$ and $\alpha = 1$, are shown on Table 1.

5.4

Template genetics: signatures and clones

An examination of Table 1 should convince the reader that template coefficients uniquely define an element once and for all, although the use of author-assigned acronyms has been prevalent in the FE literature. The parameter set can be likened to an “element genetic fingerprint” or “element DNA” that makes it a unique object. This set is called the element *signature*.

Table 1. Template signatures of some existing KPT elements

Acronym	α	β_{1j}	β_{2j}	β_{3j}	β_{4j}	β_{5j}	β_{6j}	β_{7j}	β_{8j}	β_{9j}	β_{sc}
ALR	0	-3	0	0	0	0	0	0	3	0	/2
		-6	0	0	0	0	0	0	0	0	
		0	0	0	0	0	0	0	0	0	
		0	0	0	0	0	0	0	-6	0	
AQR0	0	Same β s as AQR1									
AQRBE	$1/\sqrt{2}$	Same β s as AQR1									
AQR1	1	-3	0	0	0	0	0	0	3	0	/2
		-2	0	0	0	0	0	0	0	0	
		0	0	0	0	0	0	0	0	-4	
		0	0	0	0	0	0	0	-2	0	
AVG	0	-3	0	0	0	0	0	0	3	0	/2
BCIZ0	0	-3	1	1	0	0	-1	-1	3	0	/2
BCIZ1	1	-3	0	0	-1	1	0	0	3	0	/2
		0	0	0	2	0	0	2	0	0	
		0	0	-2	0	0	-2	0	0	0	
		0	2	0	0	2	0	0	0	0	
DKT	1	-6	1	1	-2	2	-1	-1	6	0	/4
		0	0	0	4	0	0	-2	0	0	
		0	0	2	0	0	2	0	0	0	
		0	-2	0	0	4	0	0	0	0	
FF0	0	-9	1	1	-2	2	-1	-1	9	0	/6
FF1	1	Same β s as FF0									
HCT	1	-11	5	0	-2	2	0	-5	11	0	/4
		6	0	0	4	0	0	10	0	0	
		0	0	20	0	0	20	0	0	0	
		0	10	0	0	4	0	0	6	0	

Table 2. Element identifiers used in Table 1

Name	Description
ALR	Assumed Linear Rotation KPT element of Militello and Felippa (1991)
AQR1	Assumed Quadratic Rotation KPT element of Militello and Felippa (1991)
AQR0	α -variant of AQR1 with $\alpha = 0$
AQRBE	α -variant of AQR1 with $\alpha = 1/\sqrt{2}$; of interest because it is BME.
AVG	Average curvature KPT element of Militello and Felippa (1991)
BCIZ0	Nonconforming element of Bazeley, Cheung, Irons and Zienkiewicz (1966) “sanitized” with $\alpha = 0$ as described by Felippa, Haugen and Militello (1995). Historically the first polynomial-based, complete, nonconforming KPT and the motivation for the original (multielement) patch test of Irons. See Section 5.4 for two clones of BCIZ0.
BCIZ1	Variant of above, in which the original BCIZ is sanitized with $\alpha = 1$
DKT	Discrete Kirchhoff Triangle of Stricklin et al. (1969), streamlined by Batoz (1982); see also Bathe, Batoz and Ho (1980)
FF0	Free-formulation element of Felippa and Bergan (1987).
FF1	α variant of FF0 with $\alpha = 1$.
HCT	Hsieh-Clough-Tocher element (Clough and Tocher, 1966) with curvature field collocated at the 3 midpoints. The original (macroelement) version was the first successful C^1 conforming KPT.

Table 3. Linear constraints for KPT-1-36 template

ARI2:	$\beta_{11} = (2\beta_{10} + \beta_{20} + 3\beta_{30} - 4\beta_{40})/3, \beta_{22} = (8\beta_{20} - 4\beta_{30} + 2\beta_{40})/9$
ARI1:	$\beta_{33} = \beta_{20} - \beta_{30} - \beta_{22}, \beta_{92} = 2\beta_{10} + \beta_{20} + 3\beta_{30} - 4\beta_{40} - \beta_{11}$
ARI1:	$\beta_{23} = -2\beta_{20} + \beta_{22}, \beta_{32} = 2\beta_{30} + \beta_{33}, \beta_{41} = -2\beta_{40} - \beta_{33}$
ARI1:	$\beta_{12} = \beta_{22}, \beta_{93} = \beta_{33}, \beta_{13} = -\beta_{33}, \beta_{82} = \beta_{22}, \beta_{43} = -\beta_{33}$
ARI0:	$\beta_{21} = \beta_{31} = \beta_{42} = \beta_{52} = \beta_{63} = \beta_{73} = 0$
ENO1:	$\beta_{32} = \beta_{23} + \beta_{41}, \beta_{92} = 2\beta_{11} - \beta_{12} + \beta_{82}, \beta_{13} = -\beta_{82} + \beta_{93}, \beta_{33} = \beta_{22} + \beta_{43}$
ENO0:	$\beta_{40} = -\beta_{20} - \beta_{30}$
OI1:	$\beta_{51} = \beta_{52} + \beta_{43} - \beta_{42}, \beta_{53} = \beta_{52} - \beta_{42} + \beta_{41}, \beta_{61} = \beta_{63} - \beta_{31} + \beta_{33},$
OI1:	$\beta_{62} = \beta_{63} + \beta_{32} - \beta_{31}, \beta_{71} = \beta_{73} - \beta_{21} + \beta_{23}, \beta_{72} = \beta_{73} - \beta_{21} + \beta_{22},$
OI1:	$\beta_{81} = \beta_{82} - \beta_{12} + \beta_{13}, \beta_{83} = \beta_{82} - \beta_{12} + \beta_{11}, \beta_{91} = \beta_{93}$
OI0:	$\beta_{50} = -\beta_{40}, \beta_{80} = -\beta_{10}, \beta_{60} = -\beta_{30}, \beta_{70} = -\beta_{20}, \beta_{90} = 0$

If signatures were randomly generated, the number of element instances would be of course huge: more precisely ∞^{37} for 37 parameters. But in practice elements are not fabricated at random. Attractors emerge. Some element derivation methods, notably those based on displacement shape functions, tend to “hit” certain signature patterns. The consequence is that the same element may be discovered separately by different authors, often using dissimilar derivation techniques. Such elements will be called *clones*. Cloning seems to be more prevalent among instances of the order-zero KPT-1-9 template (8). Some examples discovered in the course of this study are reported.

The first successful nonconforming triangular plate bending element was the original BCIZ (Bazeley et al., 1966). This element, however, does not pass the IET, and in fact fails Irons’ original patch test for arbitrary mesh patterns. The cause of the disease resides in the basic stiffness. The element can be “sanitized” by removing the infected matrix as described by Felippa, Haugen and Militello (1995). This is replaced by a healthy K_b with, for example, $\alpha = 0$ or $\alpha = 1$. This transplant operation yields the elements called BCIZ0 and BCIZ1, respectively, in Table 1. [These are two instances of a $BCIZ(\alpha)$ family.] Note that BCIZ0 pertains to the KPT-1-9 template.

In the 3rd MAFELAP Conference, Hansen, Bergan and Syversten (1978) reported a nonconforming element which passed the IET and (for the time) was of competitive

performance. Construction of its template signature revealed it to be a clone of BCIZ0. The plate bending part of the TRIC shell element (Argyris, Tenek and Olofsson, 1997) is also a clone of BCIZ0.

An energy orthogonal version of the HBS element was constructed by Nygård in his Ph.D. thesis (Nygård, 1986). Its signature turned out to agree with that of the FF0 element, constructed by Felippa and Bergan (1987) with a different set of higher order shape functions.

Clones seem rarer in the realm of the full KPT-1-36 template because of its greater richness. The DKT appears to be an exception. Although this popular element is usually constructed by assuming rotation fields, it coalesced with one of the ANDES elements derived by Militello and Felippa (1991). At the time the coalescence was suspected from benchmarks, and later verified by direct examination of stiffness matrices. Using the template formulation such numerical tests can be bypassed, as it is sufficient to compare signatures.

5.5 Parameter constraints

To construct element families and in the limit, specific elements, constraints on the free parameters must be imposed. One key difficulty surfaces. Constraints must be imposed at the *local* level of individual element or simple mesh units, but they should lead to high performance

behavior at the *global* level. There is as yet no mathematical framework for establishing those connections.

Several constraint types have been used in this and previous work: (1) invariance, (2) skewness and aspect ratio insensitivity, (3) distortion insensitivity, (4) truncation error minimization, (5) energy balance, (6) energy orthogonality, (7) morphing. Whereas (1) and (2) have clear physical significance, the effect of the others has to be studied empirically on benchmark problems. Conditions that have produced satisfactory results are discussed below with reference to the KPT template. The reader should be cautioned, however, that these may not represent the final word inasmuch as templates are presently a frontier subject. For convenience the constraints can be divided into linear and nonlinear, the former being independent of constitutive properties.

5.6

Staged element design

Taking an existing KPT element that passes the IET and finding its template signature is relatively straightforward with the help of a computer algebra program. Those listed in Table 1 were obtained using *Mathematica*. But in element design we are interested in the reverse process: starting from a general template such as KPT-1-36, to arrive at specific elements that display certain desirable characteristics. Experience shows that this is best done in two stages.

First, linear constraints on the free parameters are applied to generate *element families*. The dependence on the remaining free parameters is still linear.

Second, selected energy balance constraints are imposed. For linear elastic elements such constraints are quadratic in nature. Consequently there is no guarantee that real solutions exist. If they do, solutions typically produce families with few (usually 1 or 2) free parameters; in particular α families. Finally, setting the remaining parameters to specific values produces element instances.

6

Linear constraints

Three types of linear constraints have been used to generate element families.

6.1

Observer invariance (OI) constraints

These pertain to *observer invariance*. If the element geometry exhibits symmetries, those must be reflected in the stiffness equations. For example, if the triangle becomes equilateral or isosceles, certain equality conditions between entries of the curvature-displacement matrices must hold. The resulting constraints are *linear* in the β s.

For the KPT-1-36 template one obtains the 14 constraints labeled as OI0 and OI1 in Table 3. The five OI0 constraints pertain to the order zero parameters and would be the only ones applicable to the KPT-1-9 template. They can be obtained by considering an equilateral triangle. The nine OI1 constraints link parameters of order one. This constraint set must be the first imposed and applies to any element.

6.2

Aspect ratio insensitivity (ARI) constraints

A second set of constraints can be found by requiring that the element be *aspect ratio insensitive*, or ARI for short, when subjected to arbitrary node displacements. A triangle that violates this requirement becomes infinitely stiff for certain geometries when a certain dimension aspect ratio r goes to infinite.

To express this mathematically, it is sufficient to consider the triangle configurations (A, B, C) depicted in Fig. 1. In all cases L denotes a triangle dimension kept fixed while the aspect ratio r is increased. In configuration A, the angle ψ is kept fixed as $r \rightarrow \infty$. The opposite angles tend to zero and $\pi/2 - \psi$. The case $\psi = 90^\circ = \pi/2$ is particularly important as discussed later. In configurations (B) and (C) the ratio ξ is kept fixed as $r \rightarrow \infty$, and angles tend to π , $\pi/2$ or zero.

As higher order test displacements we select the four cubic modes $w_{30} = x^3$, $w_{21} = x^2y$, $w_{12} = xy^2$ and $w_{03} = y^3$. Any other cubic mode is a combination of those four. Construct the element energy ratios defined in Section 4.3. The important dependence of those ratios on physical properties and free parameters is

$$\rho = \rho_b^m(r, \psi, \alpha) + \rho_h^m(r, \psi, \beta_j) \quad (9)$$

where $m = 30, 21, 12, 03$ identifies modes x^3 , x^2y , xy^2 and y^3 , respectively. (The dependence on L and D is innocuous for this study and omitted for simplicity). Take a particular configuration (A, B, C) and mode m , and let $r \rightarrow \infty$. If ρ remains nonzero and bounded the element is said to be *aspect ratio insensitive* for that combination. If $\rho \rightarrow \infty$ the element is said to experience *aspect ratio locking*, whereas if $\rho \rightarrow 0$ the element becomes infinitely flexible. If ρ remains nonzero and bounded for all modes and configurations the element is called *completely aspect ratio insensitive*. The question is whether free parameters can be chosen to attain this goal.

As posed an answer appears difficult because the ratios (9) are quadratic in the free parameters, rational in r , and transcendental in ψ . Fortunately the question can be reduced to looking at the dependence of the curvature-dis-

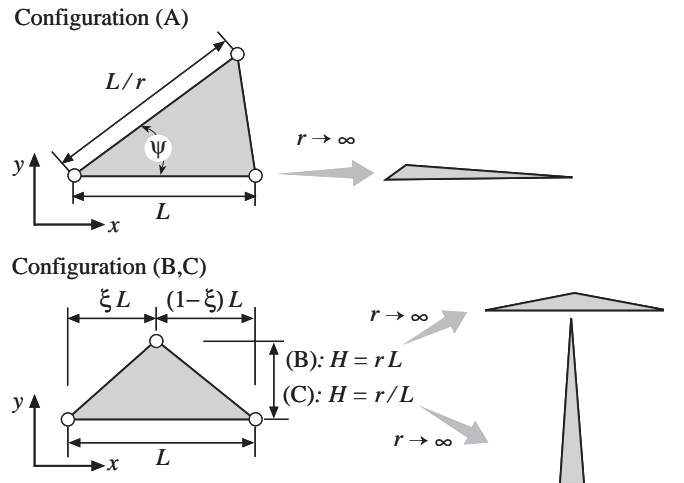


Fig. 1. Triangle configurations for the study of ARI constraints

placement matrices on r as $r \rightarrow \infty$. Entries of these matrices are linear functions of the free parameters. As $r \rightarrow \infty$ no entry must grow faster than r [because exact curvatures grow as $O(r)$]. For example, if an entry grows as r^2 , setting its coefficient to zero provides a linear constraint from which the dependence on L and ψ is factored out. The material properties do not come in. Even with this substantial simplification the use of a CAS is mandatory to handle the elaborate symbolic algebra involved, which involves the Laurent expansion of all curvature matrices. The result of the investigation for the KPT-1-36 template can be summarized as follows.

- (1) The basic energy ratio ρ_b is bounded for all ψ and all m in configuration (A). In configurations (B) and (C) it is unbounded as $O(r)$ in two cases: $m = 30$ if $\alpha \neq 1$, and $m = 21$ for any α .
- (2) The higher order energy ratio ρ_h can be made bounded for all ψ and m by imposing the 18 linear constraints listed in Table 3 under the ARI label.
- (3) The foregoing bound on ρ_h is not possible for the KPT-1-9 template. Thus a signature of the form (8) is undesirable from a ARI standpoint.

Because of the basic stiffness shortcoming noted in (1), a completely ARI element cannot be constructed. However, the β s can be selected to guarantee that ρ_h is always bounded. The resulting constraints are listed in Table 3. They are grouped in three subsets labeled ARI0, ARI1 and ARI2.

Subset ARI0 requires $\beta_{21} = \beta_{31} = \beta_{42} = \beta_{52} = \beta_{63} = \beta_{73} = 0$. If any of these 6 parameters is nonzero, one or more entries of the deviatoric curvature displacement matrices grow as r^3 in the 3 configurations. This represents disastrous aspect ratio locking and renders any such element useless.

Once OI0, OI1 and ARI0 are imposed, subset ARI1 groups 10 constraints obtained by setting to zero $O(r^2)$ grow in configuration (A) for all HO modes. This insures that $\rho = \rho_b + \rho_h$ stays bounded in that configuration (because ρ_b stays bounded for any α). In Table 3 they are listed in reverse order of that found by the symbolic

analysis program, which means that the most important ones appear at the end.

Once OI0, OI1 and ARI0 and ARI1 are imposed, the 2-constraint subset ARI2 guarantees that ρ_h is bounded for configurations (B) and (C). Since ρ_b is not necessarily bounded in this case these conditions have minor practical importance.

Imposing OI0, OI1, ARI0 and ARI1 leaves $37 - 5 - 9 - 6 - 10 = 7$ free parameters, and produces the so-called ARI family defined in Table 4. Of the seven parameters, four are chosen to be the actual template parameters α , β_{10} , β_{20} , and β_{30} . Three auxiliary parameters, called γ_1 , γ_2 and γ_3 , are chosen to complete the generation of the ARI family as defined in Table 4.

This family is interesting in that it includes all existing high-performance elements, such as DKT and AQR1, as well as some new ones developed in the course of this study.

6.3

Energy orthogonality (ENO) constraints

Energy orthogonality (ENO) means that the average value of deviatoric strains over the element is zero. Mathematically, $\mathbf{B}_{\gamma 4} + \mathbf{B}_{\gamma 5} + \mathbf{B}_{\gamma 6} = \mathbf{0}$. This condition was a key part of the early developments of the Free Formulation by Bergan (1980) and Bergan and Nygård (1984) as well as of elements developed during the late 1980s and early 1990s.

The heuristic rationale behind ENO is to limit or preclude energy coupling between constant strain and higher order modes. A similar idea lurks behind the so-called ‘‘B-bar’’ formulation, which has a long and checkered history in modeling incompressibility and plastic flow.

For the KPT-1-36 element one may start with the OI0 and OI1 constraints as well as ARI0 (to preclude catastrophic locking), but ignoring ARI1 and ARI2. Then the ENO condition leads to the linear constraints labeled as ENO0 and ENO1 in Table 3. These group conditions on the order zero and one parameters, respectively. Imposing OI0, OI1, ARI0, ENO0 and ENO1 leads to the ENO family defined in Table 4, which has 12 free parameters. Elements ALR, FF0 and FF1 of Table 1 can be presented as instance of this family as shown in Table 7.

Table 4. Three element families derivable from KPT-1-36

ARI(α , β_{10} , β_{20} , β_{30} , γ_0 , γ_1 , γ_2)	α	β_{10}	β_{20}	β_{30}	β_{40}	$-\beta_{40}$	β_{30}	$-\beta_{20}$	$-\beta_{10}$	0
		β_{11}	0	0	β_{41}	$-\beta_{61}$	β_{61}	β_{71}	$-\beta_{61}$	β_{61}
		β_{22}	β_{22}	β_{62}	0	0	β_{62}	β_{22}	β_{22}	β_{92}
		$-\beta_{61}$	β_{71}	β_{61}	$-\beta_{61}$	β_{41}	0	0	β_{11}	β_{61}

where $\beta_{40} = -\beta_{20} - \beta_{30} + \gamma_0$, $\beta_{11} = (2\beta_{10} + \beta_{20} + 3\beta_{30} - 4\beta_{40})/3 + \gamma_1$,
 $\beta_{22} = (8\beta_{20} - 4\beta_{30} + 2\beta_{40})/9 + \gamma_2$, $\beta_{61} = \beta_{20} - \beta_{22} - \beta_{30}$, $\beta_{41} = -\beta_{61} - 2\beta_{40}$,
 $\beta_{62} = \beta_{20} - \beta_{22} + \beta_{30}$, $\beta_{71} = -2\beta_{20} + \beta_{22}$ and $\beta_{92} = 2\beta_{10} - \beta_{11} + \beta_{20} + 3\beta_{30} - 4\beta_{40}$.

ENO(α , β_{10} , β_{20} , β_{30} , β_{11} , β_{41} , β_{12} , β_{22} , β_{82} , β_{23} , β_{43} , β_{93})	α	β_{10}	β_{20}	β_{30}	β_{40}	$-\beta_{40}$	$-\beta_{30}$	$-\beta_{20}$	$-\beta_{10}$	0
		β_{11}	0	0	β_{41}	β_{43}	β_{33}	β_{23}	β_{81}	β_{93}
		β_{12}	β_{22}	β_{32}	0	0	β_{32}	β_{22}	β_{82}	β_{92}
		β_{13}	β_{23}	β_{33}	β_{43}	β_{41}	0	0	β_{83}	β_{93}

where $\beta_{40} = -\beta_{20} - \beta_{30}$, $\beta_{81} = -\beta_{12} + \beta_{93}$, $\beta_{32} = \beta_{23} + \beta_{41}$, $\beta_{92} = 2\beta_{11} - \beta_{12} + \beta_{82}$,
 $\beta_{13} = -\beta_{82} + \beta_{93}$, $\beta_{33} = \beta_{22} + \beta_{43}$ and $\beta_{83} = \beta_{11} - \beta_{12} + \beta_{82}$.

ARIENO(α , β_{10} , β_{20} , β_{30})	ARI(α , β_{10} , β_{20} , β_{30} , 0, 0, 0)
---	---

If instead one starts from the ARI family it can be verified that ENO is obtained if $\gamma_0 = \gamma_1 = \gamma_2 = 0$; that is, only three constraints are needed instead of five. [This is precisely the rationale for selecting those “ENO deviations” as free arguments]. Moreover, the order-one constraints $\gamma_1 = \gamma_2 = 0$ are precisely ARI2 in disguise.

Setting $\gamma_0 = \gamma_1 = \gamma_2 = 0$ in ARI yields a four-parameter family called ARIENO (pronounced like the French “Arienne”). The free parameters are α , β_{10} , β_{20} and β_{30} . Its template is defined in Table 4. As noted, this family incorporates all constraints listed in Table 3. (These adds up to 37 but there are 4 redundancies.)

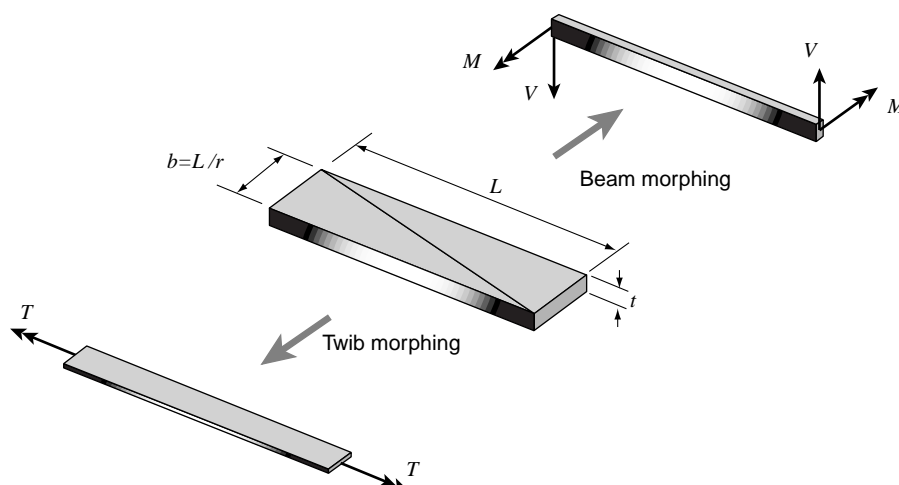
As noted all high performance elements found to date are ARI. Most are ENO, but there are some that are not. One example is HCTS, a “smoothed HCT” element developed in this study. Hence circumstantial evidence suggests that ARI is more important than ENO. In the present investigation ENO is used as a guiding principle rather than an *a priori* constraint.

7

Quadratic constraints

As noted in the foregoing section, the ARI family – and its ARIENO subset – is a promising source of high performance KPT elements. But seven parameters remain to be set to meet additional conditions. Such conditions fall into the general class of *energy balance* constraints introduced by Bergan and Felippa (1985). Unit energy ratios are imposed for specific mesh unit geometries, loading and boundary conditions. The common feature of such constraints is that (for linear elements) they are *quadratic* in the free parameters, and involve the constitutive properties. Because of the quadratic character, real parameter solutions are not guaranteed. Even if they have real solutions, the resulting families may exist only for limited parameter ranges.

Numerous variants of the energy balance tests have been developed over the years. Because of space constraints only three variations under study are described below. All of them have immediate physical interpretation in terms of the design of custom elements. They have been applied assuming isotropic material with zero Poisson’s ratio.



7.1

Morphing constraints

This is a class of constraints that is presently being studied to ascertain whether enforcement would be generally beneficial to element performance. Consider the 2-KPT-element rectangular mesh unit shown in the center of Fig. 2. The aspect ratio r is the ratio of the longest rectangle dimension L to the width $b = L/r$. The plate is fabricated of a homogeneous isotropic material with zero Poisson’s ratio and thickness t . Axis x is selected along the longitudinal direction. We study the two *morphing processes* depicted in Fig. 2. In both cases the aspect ratio r is made to increase, but with two different objectives.

Plane Beam Limit. The width $b = L/r$ is decreased while keeping L and t fixed. The limit is the thin, Bernoulli-Euler plane beam member of rectangular cross section $t \times b$, $b \ll t$, shown on the right of Fig. 2. This member can carry exactly a linearly-varying bending moment $M(x)$ and a constant transverse shear V , although shear deformations are not considered.

Twib Limit. Again the width $b = L/r$ is decreased by making r grow. The thickness t , however, is still considered small with respect to b . The limit is the twisted-ribbon member of narrow cross section $t \times b$, $t \ll b$, shown on the left of Fig. 2. This member, called a “twib” for brevity, can carry a longitudinal torque $T(x)$. This torque may vary linearly in x .

Conditions called *morphing constraints* are now posed as follows.

- (1) Does the mesh unit approach the exact behavior of a Hermitian (cubic) beam? If so, the plate element is said to be *beam morphing exact* or BE for short.
- (2) Does the mesh unit approach the exact beam behavior as both $r \rightarrow \infty$ and $r \rightarrow 0$? If so, the plate element is said to be *double beam morphing exact* or DBE for short.
- (3) Does the mesh unit approach the exact behavior of a twib under linearly varying torque? If so, the plate element is said to be *twib-morphing-exact* or TME.

The BE and TE conditions can be derived by symbolically expanding transformed mesh-unit stiffness equations in Laurent series as $r \rightarrow \infty$. The DBME condition requires

Fig. 2. Morphing a rectangular plate mesh unit to beam and twib

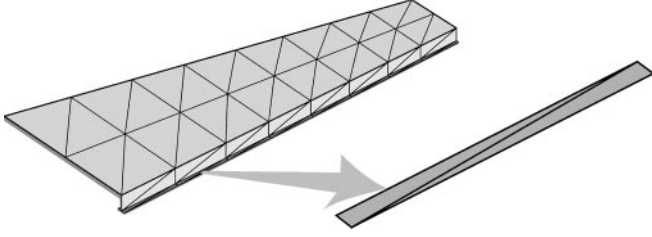


Fig. 3. Stiffened panels modeled by facet shell elements are a common source of high aspect ratio elements

also a Taylor expansion as $r \rightarrow 0$. They can also be derived as asymptotic forms of energy ratios.

An element satisfying (1) and (3) is called BTE, and one satisfying (1), (2) and (3) is called DBTE. The practical interest for morphing conditions is the appearance of very high aspect ratios in modeling certain aerospace structures such as the stiffened panel depicted in Fig. 3.

7.2

Mesh direction insensitivity constraints

This class of constraints is important in high frequency dynamics to minimize mesh induced dispersion. Consider a square mesh unit fabricated of 4 overlapped triangles to try to minimize directionality from the start. Place Carte-

sian axes x and y at the mesh unit center. Apply higher order modes \bar{x}^3 and $\bar{x}^2\bar{y}$ where \bar{x} forms an angle φ with x , and require that $\rho = 1$ for all φ . Starting from ARIENO one can construct α families which satisfy that constraint. The simplest one is the MDIT(α) family, which for $\alpha = 1$ yields the element MDIT1 defined in Table 5.

7.3

Distortion minimization constraints

An element is distortion insensitive when the solution hardly changes even when the mesh is significantly changed. Precise quantification of this definition in terms of energy ratios on standard benchmarks tests is presently under study. Preliminary conclusions suggest that sensitivity to distortion is primarily controlled by the basic stiffness parameter α whereas the β s only play a secondary role. For the KPT templates $\alpha = 1$ appears to minimize the distortion sensitivity.

8

New KPT elements

Starting from the ARI family and applying various energy constraints, a set of new elements with custom properties have been developed in this study. The most promising ones are summarized in Tables 5 and 6. Table 7 gives the

Table 5. Template signatures of selected new KPT elements

Acronym	α	β_{1j}	β_{2j}	β_{3j}	β_{4j}	β_{5j}	β_{6j}	β_{7j}	β_{8j}	β_{9j}	β_{sc}
BTE13	1/3	-9 -5 2 -1	2 0 2 -2	-1 0 -1 1	-1 1 0 -1	1 -1 0 1	1 1 -1 0	-2 -2 2 0	9 -1 2 -5	0 1 -10 1	/6
DBE00	ARIENO(0, -3/2, β_{20} , β_{30}), with $\beta_{20} = 3(\sqrt{6} - 2)/4$ and $\beta_{30} = -\beta_{20}$.										
DBE13	ARIENO(1/3, -3/2, β_{20} , β_{30}) with $\beta_{20} = -3/2 - (\sqrt{25 - \sqrt{609}})/12 + (25 + \sqrt{609})/4$ and $\beta_{30} = 3/2 - (\sqrt{25 - \sqrt{609}})/12 - (25 + \sqrt{609})/4$.										
DBE12	ARIENO(1/2, -3/2, β_{20} , β_{30}) with $\beta_{20} = (-12 - \sqrt{10 - 2\sqrt{21}} + 3\sqrt{10 + 2\sqrt{21}})/8$ and $\beta_{30} = (12 - \sqrt{10 - 2\sqrt{21}} - 3\sqrt{10 + 2\sqrt{21}})/8$.										
DBEN00	0	-3 2 0 0	0 0 0 0	0 0 0 0	0 0 0 0	0 0 0 0	0 0 0 0	0 0 0 0	3 0 0 2	0 0 -8 0	/2
DBEN13	1/3	-27 $4\sqrt{61} - 22$ 0 0	-1 0 2 0	-1 0 0 0	2 -4 0 0	-2 0 -4 0	1 0 0 0	1 2 0 0	27 0 0 $4\sqrt{61} - 22$	0 0 0 0	/18
DBEN12	1/2	-12 $4(\sqrt{6} - 3)$ 0 0	-1 0 0 2	-1 0 -2 0	2 -4 0 0	-2 0 0 -4	1 0 -2 0	1 2 0 0	12 0 0 $4(\sqrt{6} - 3)$	0 0 -4($\sqrt{6} + 6$) 0	/8
DBTE13	ARIENO(1/3, -1.3100926, 0.40467862, -0.49926464)										
HCTS	1	-18 8 0 0	5 0 0 -10	5 0 10 0	-1 2 0 0	1 0 0 2	-5 0 10 0	-5 -10 0 0	18 0 0 8	0 0 -20 0	/12
MDIT1	1	-45 -34 8 -4	6 0 8 -4	-6 0 8 4	0 -4 0 -4	0 -4 0 -4	6 4 -8 0	-6 -4 8 0	45 -4 8 -34	0 4 8 4	/30

Table 6. Brief description of new elements listed in Table 5

Name	Description
BTE13	Instance of the BTE(α) family for $\alpha = 1/3$. This is a subset of ARIENO which exhibits beam morphing and twib morphing exactness in the sense discussed in Section 7.1.
DBE00, DBE13, DBE12	Instances of the DBE(α) family for $\alpha = 0$, $\alpha = 1/3$ and $\alpha = 1/2$, respectively. This family is a subset of ARIENO which exhibits double-beam morphing exactness. The DBE family exists (in the sense of having real solutions) for $\alpha \leq 1/\sqrt{2}$.
DBEN00, DBEN13, DBEN12	Instances of the DBEN(α) family for $\alpha = 0$, $\alpha = 1/3$ and $\alpha = 1/2$, respectively. This family exhibits double-beam morphing exactness but is not ENO. It exists for $\alpha \leq 1/\sqrt{2}$.
DBTE13	An ARIENO instance with $\alpha = 1/3$ which exhibits double-beam morphing and twib morphing exactness. It was found by minimizing a residual function. Only numerical values for the coefficients are known. Such elements appear to exist only for a small α range.
HCTS	An element derived from the HCT, which is a too-stiff poor performer, by smoothing its curvature field. It displays very high performance if beam or twib exactness is not an issue. Member of ARI but not ARIENO.
MDIT1	Instance of the MDIT(α) family for $\alpha = 1$. MDI stands for Mesh-Direction Insensitive. Such elements display stiffness isotropy when assembled in a square mesh unit. Primarily of interest in high frequency dynamics. Static performance good but not outstanding.

10

Table 7. Genealogy of specific KPT elements

Name	Source Family
ALR	ARI (0, -3/2, 0, 0, 0, -2, 0)
AQR1	ARIENO (1, -3/2, 0, 0)
AQR0	ARIENO (0, -3/2, 0, 0)
AQRBE	ARIENO (1/√2, -3/2, 0, 0)
AVG	ENO (0, -3/2, 0, 0, 0, 0, 0, 0, 0, 0)
BCIZ0 (and clones), BCIZ1, HCT	Not ARI or ENO
BTE13	ARIENO (1/3, -3/2, 1/3, -1/6)
DBE00, DBE13, DBE12	See Table 5
DBEN00	ARI (0, -3/2, 0, 0, 0, 2, 0)
DBEN13	ARI (0, -3/2, -1/18, -1/18, 0, 2√61/9, 0)
DBEN12	ARI (0, -3/2, -1/8, -1/8, 0, √3/2, 0)
DKT	ARIENO (1, -3/2, 1/4, 1/4)
FF0 (and clones)	ENO (0, -3/2, 1/6, 1/6, 0, 0, 0, 0, 0, 0)
FF1	ENO (1, -3/2, 1/6, 1/6, 0, 0, 0, 0, 0, 0)
HCTS	ARI (1, -3/2, 5/12, 5/12, 3/4, 1, -1/6)
MDIT1	ARIENO (1, -3/2, 1/5, -1/5)

genealogy (in the sense of element family membership) of all elements listed in Tables 1 and 6.

The performance of the old and new elements in a comprehensive set of plate bending benchmarks is still in progress, and will be reported in a sequel paper. It should be noted that the unification brought about by the template approach is very beneficial for such comparisons, because all possible elements of a given type and node/freedom configuration can be implemented with a single program module.

9

Conclusions

The usual finite element construction process, which involves *a priori* selection of a variational principle and shape functions, hinders the exploration of a wide range of admissible finite element models. As such it is ineffectual for the *design* of finite elements with desirable physical behavior. The application described here illustrates the

effectiveness of templates to build custom elements. The template approach attempts to implement the hope long ago expressed by Bergan and Hansen (1975) in the Introduction of their MAFELAP II paper:

“An important observation is that each element is, in fact, only represented by the numbers in its stiffness matrix during the analysis of the assembled system. The origin of these stiffness coefficients is unimportant to this part of the solution process ... The present approach is in a sense the opposite of that normally used in that the starting point is a generally formulated convergence condition and from there the stiffness matrix is derived ... The patch test is particularly attractive [as such a condition] for the present investigation in that it is a direct test on the element stiffness matrix and requires no prior knowledge of interpolation functions, variational principles, etc.”

This statement sets out what may be called the *direct algebraic approach* to finite elements: the element stiffness is derived directly from consistency conditions – provided by the Individual Element Test – plus stability and accuracy considerations to determine algebraic redundancies if any. It has in fact many points in common with energy-based finite differences.

This ambitious goal has proven elusive because the direct algebraic construction of the stiffness matrix of most multidimensional elements becomes effectively a problem in constrained optimization. In the *symbolic form* necessitated by element design, such problem is much harder to tackle than the conventional element construction method based on shape functions. Only with the advent and general availability of powerful computer algebra systems can the dream become a reality.

Appendix A

Formulation of KPT-1-36 template

This Appendix collects the formulas that fully define the KPT-1-36 element template.

A1

Element relations

The triangle geometry is defined by the corner coordinates in its (x, y) local system, which are (x_i, y_i) , $i = 1, 2, 3$.

Coordinate differences are abbreviated as $x_{ij} = x_i - x_j$ and $y_{ij} = y_i - y_j$. The signed triangle area A is given by $2A = x_{21}y_{31} - x_{31}y_{21} = x_{32}y_{12} - x_{12}y_{32} = x_{13}y_{23} - x_{23}y_{13}$ and we require that $A > 0$. The visible degrees of freedom of the element collected in \mathbf{u} and the associated node forces collected in \mathbf{f} are

$$\mathbf{u}^T = [u_{z1} \ \theta_{x1} \ \theta_{y1} \ u_{z2} \ \theta_{x2} \ \theta_{y2} \ u_{z3} \ \theta_{x3} \ \theta_{y3}] . \quad (10)$$

$$\mathbf{f}^T = [f_{z1} \ \mathcal{M}_{x1} \ \mathcal{M}_{y1} \ f_{z2} \ \mathcal{M}_{x2} \ \mathcal{M}_{y2} \ f_{z3} \ \mathcal{M}_{x3} \ \mathcal{M}_{y3}] . \quad (11)$$

The Cartesian components of the plate curvatures are κ_{xx} , κ_{yy} and $2\kappa_{xy} = \kappa_{xy} + \kappa_{yx}$, which are gathered in a 3-vector κ . In the Kirchhoff model, curvatures and displacements are linked by

$$\kappa_{xx} = \frac{\partial^2 w}{\partial x^2}, \quad \kappa_{yy} = \frac{\partial^2 w}{\partial y^2}, \quad 2\kappa_{xy} = 2 \frac{\partial^2 w}{\partial x \partial y} . \quad (12)$$

$$\kappa = \begin{bmatrix} \frac{\partial^2 w}{\partial x^2} \\ \frac{\partial^2 w}{\partial y^2} \\ 2 \frac{\partial^2 w}{\partial x \partial y} \end{bmatrix} = \frac{1}{4A^2} \begin{bmatrix} y_{23}y_{13} & y_{31}y_{21} & y_{12}y_{32} \\ x_{23}x_{13} & x_{31}x_{21} & x_{12}x_{32} \\ y_{23}x_{31} + x_{32}y_{13} & y_{31}x_{12} + x_{13}y_{21} & y_{12}x_{23} + x_{21}y_{32} \end{bmatrix} \begin{bmatrix} \frac{\partial^2 w}{\partial \pi_{21}^2} \\ \frac{\partial^2 w}{\partial \pi_{32}^2} \\ \frac{\partial^2 w}{\partial \pi_{13}^2} \end{bmatrix} = \mathbf{T} \chi . \quad (15)$$

where $w = w(x, y) \equiv u_z$ is the plate transverse displacement. In the KPT elements considered here, however, the compatibility equations (12) must be understood in a weak sense because the assumed curvature field is not usually integrable. The internal moment field is defined by the Cartesian components m_{xx} , m_{yy} and m_{xy} , which are placed in a 3-vector \mathbf{m} . Curvatures and moments are linked by the constitutive relation

$$\mathbf{m} = \begin{bmatrix} m_{xx} \\ m_{yy} \\ m_{xy} \end{bmatrix} = \begin{bmatrix} D_{11} & D_{12} & D_{13} \\ D_{12} & D_{22} & D_{23} \\ D_{13} & D_{23} & D_{33} \end{bmatrix} \begin{bmatrix} \kappa_{xx} \\ \kappa_{yy} \\ 2\kappa_{xy} \end{bmatrix} = \mathbf{D} \kappa . \quad (13)$$

where \mathbf{D} results from integration through the thickness in the usual way. Three dimensionless side direction coordinates

π_{21} , π_{32} and π_{13} are defined as going from 0 to 1 by marching along sides 12, 23 and 31, respectively. The side coordinate π_{ji} of a point not on a side is that of its projection on side ij . The second derivatives of $w \equiv u_z$ with respect to the dimensionless side directions will be called the *natural curvatures* and are denoted by $\chi_{ji} = \partial^2 w / \partial \pi_{ji}^2$. These curvatures have dimensions of displacement. They are related to the Cartesian plate curvatures by the matrix relation

$$\chi = \begin{bmatrix} \chi_{21} \\ \chi_{32} \\ \chi_{13} \end{bmatrix} = \begin{bmatrix} \frac{\partial^2 w}{\partial \pi_{21}^2} \\ \frac{\partial^2 w}{\partial \pi_{32}^2} \\ \frac{\partial^2 w}{\partial \pi_{13}^2} \end{bmatrix} = \begin{bmatrix} x_{21}^2 & y_{21}^2 & x_{21}y_{21} \\ x_{32}^2 & y_{32}^2 & x_{32}y_{32} \\ x_{13}^2 & y_{13}^2 & x_{13}y_{13} \end{bmatrix} \begin{bmatrix} \frac{\partial^2 w}{\partial x^2} \\ \frac{\partial^2 w}{\partial y^2} \\ 2 \frac{\partial^2 w}{\partial x \partial y} \end{bmatrix} = \mathbf{T}^{-1} \kappa , \quad (14)$$

the inverse of which is

The transformation equations (14) and (15) are assumed to hold even if $w(x, y)$ is only known in a weak sense.

A2

The basic stiffness template

Following Militello and Felippa (1991) the α -parametrized basic stiffness is defined as the linear combination

$$\mathbf{K}_b = A^{-1} \mathbf{L} \mathbf{D} \mathbf{L}^T, \quad \mathbf{L} = (1 - \alpha) \mathbf{L}_l + \alpha \mathbf{L}_q \quad (16)$$

where \mathbf{L} is a force-lumping matrix that maps an internal constant moment field to node forces. \mathbf{L}_l and \mathbf{L}_q are called the linear and quadratic versions, respectively, of \mathbf{L} :

$$\mathbf{L}_l^T = \begin{bmatrix} 0 & 0 & y_{32} & 0 & 0 & y_{13} & 0 & 0 & y_{21} \\ 0 & x_{32} & 0 & 0 & x_{13} & 0 & 0 & x_{21} & 0 \\ 0 & y_{23} & x_{23} & 0 & y_{31} & x_{31} & 0 & y_{12} & x_{12} \end{bmatrix} \quad (17)$$

$$\mathbf{L}_q = \begin{bmatrix} c_{n21}s_{n21} - c_{n13}s_{n13} & -c_{n21}s_{n21} + c_{n13}s_{n13} & -(c_{n21}^2 - s_{n21}^2) + (c_{n13}^2 - s_{n13}^2) \\ \frac{1}{2}(c_{n21}^2 x_{12} + c_{n13}^2 x_{31}) & \frac{1}{2}(s_{n21}^2 x_{12} + s_{n13}^2 x_{31}) & s_{n21}^2 y_{21} + s_{n13}^2 y_{13} \\ -\frac{1}{2}(c_{n21}^2 y_{21} + c_{n13}^2 y_{13}) & -\frac{1}{2}(s_{n21}^2 y_{21} + s_{n13}^2 y_{13}) & -c_{n21}^2 x_{12} - s_{n13}^2 x_{31} \\ c_{n32}s_{n32} - c_{n21}s_{n21} & -c_{n32}s_{n32} + c_{n21}s_{n21} & -(c_{n32}^2 - s_{n32}^2) + (c_{n21}^2 - s_{n21}^2) \\ \frac{1}{2}(c_{n32}^2 x_{23} + c_{n21}^2 x_{12}) & \frac{1}{2}(s_{n32}^2 x_{23} + s_{n21}^2 x_{12}) & s_{n32}^2 y_{32} + s_{n21}^2 y_{21} \\ -\frac{1}{2}(c_{n32}^2 y_{32} + c_{n21}^2 y_{21}) & -\frac{1}{2}(s_{n32}^2 y_{32} + s_{n21}^2 y_{21}) & -c_{n32}^2 x_{23} - s_{n21}^2 x_{12} \\ c_{n13}s_{n13} + c_{n32}s_{n32} & -c_{n13}s_{n13} - c_{n32}s_{n32} & -(c_{n13}^2 - s_{n13}^2) + (c_{n32}^2 - s_{n32}^2) \\ \frac{1}{2}(c_{n13}^2 x_{31} + c_{n32}^2 x_{23}) & \frac{1}{2}(s_{n13}^2 x_{31} + s_{n32}^2 x_{23}) & s_{n13}^2 y_{13} + s_{n32}^2 y_{32} \\ -\frac{1}{2}(c_{n13}^2 y_{13} + c_{n32}^2 y_{32}) & -\frac{1}{2}(s_{n13}^2 y_{13} + s_{n32}^2 y_{32}) & -c_{n13}^2 x_{31} - s_{n32}^2 x_{23} \end{bmatrix} \quad (18)$$

Here c_{nji} and s_{nji} denote the cosine and sine, respectively, of the angle formed by x and the exterior normal to side $i \rightarrow j$.

Matrix L_1 was introduced by Bergan and Nygård (1984) and L_q by Militello and Felippa (1991).

A3

The higher order stiffness template

For an element of constant D , the higher order stiffness template is defined by

$$\mathbf{K}_h = \frac{A}{3} (\mathbf{B}_4^T \mathbf{D}_\chi \mathbf{B}_4 + \mathbf{B}_5^T \mathbf{D}_\chi \mathbf{B}_5 + \mathbf{B}_6^T \mathbf{D}_\chi \mathbf{B}_6) \quad (19)$$

where $\mathbf{D}_\chi = \mathbf{T}^T \mathbf{D} \mathbf{T}$ is the plate constitutive relation expressed in terms of natural curvatures and moments, and $\mathbf{B}_{\chi m}$ are the natural curvature-displacement matrices

evaluated at the midpoints $m = 4, 5, 6$ opposing corners 3, 1, 2, respectively.

These matrices are parametrized as follows. Define the geometric invariants

$$\begin{aligned} \lambda_1 &= \frac{x_{12}x_{13} + y_{12}y_{13}}{x_{21}^2 + y_{21}^2} - \frac{1}{2}, & \lambda_2 &= \frac{x_{23}x_{21} + y_{23}y_{21}}{x_{32}^2 + y_{32}^2} - \frac{1}{2}, \\ \lambda_3 &= \frac{x_{31}x_{32} + y_{31}y_{32}}{x_{13}^2 + y_{13}^2} - \frac{1}{2}. \end{aligned} \quad (20)$$

These have a simple physical meaning as measures of triangle distortion (for an equilateral triangle, $\lambda_1 = \lambda_2 = \lambda_3 = 0$). In the following expressions, the β -derived coefficients γ_i and σ_i are selected so that the $\mathbf{B}_{\chi m}$ matrices are exactly orthogonal to all rigid body modes and constant curvature states. This is a requirement of the fundamental stiffness decomposition.

$$\begin{aligned} \beta_1 &= \beta_{10} + \beta_{11}\lambda_3 + \beta_{12}\lambda_1 + \beta_{13}\lambda_2, & \beta_2 &= \beta_{20} + \beta_{21}\lambda_3 + \beta_{22}\lambda_1 + \beta_{23}\lambda_2, & \beta_3 &= \beta_{30} + \beta_{31}\lambda_3 + \beta_{32}\lambda_1 + \beta_{33}\lambda_2, \\ \beta_4 &= \beta_{40} + \beta_{41}\lambda_3 + \beta_{42}\lambda_1 + \beta_{43}\lambda_2, & \beta_5 &= \beta_{50} + \beta_{51}\lambda_3 + \beta_{52}\lambda_1 + \beta_{53}\lambda_2, & \beta_6 &= \beta_{60} + \beta_{61}\lambda_3 + \beta_{62}\lambda_1 + \beta_{63}\lambda_2, \\ \beta_7 &= \beta_{70} + \beta_{71}\lambda_3 + \beta_{72}\lambda_1 + \beta_{73}\lambda_2, & \beta_8 &= \beta_{80} + \beta_{81}\lambda_3 + \beta_{82}\lambda_1 + \beta_{83}\lambda_2, & \beta_9 &= \beta_{90} + \beta_{91}\lambda_3 + \beta_{92}\lambda_1 + \beta_{93}\lambda_2, \\ \gamma_1 &= \beta_1 + \beta_3, & \gamma_2 &= \beta_3, & \gamma_3 &= \beta_2 + \beta_3, & \gamma_4 &= \beta_4 + \beta_9, & \gamma_5 &= \beta_9, & \gamma_6 &= \beta_6 + \beta_8, \\ \gamma_7 &= \beta_6 + \beta_7, & \gamma_8 &= \beta_6, & \gamma_9 &= \beta_5 + \beta_9, & \sigma_1 &= 2\gamma_3 - 2\gamma_1, & \sigma_2 &= 2\gamma_1, & \sigma_3 &= 2\gamma_3, \\ \sigma_4 &= 2\gamma_9 - 2\gamma_4, & \sigma_5 &= 2\gamma_4, & \sigma_6 &= -2\gamma_6, & \sigma_7 &= 2\gamma_6 - 2\gamma_7, & \sigma_8 &= 2\gamma_7, & \sigma_9 &= -2\gamma_9 \end{aligned}$$

$$\mathbf{B}_{\chi 4} = \begin{bmatrix} \sigma_5 & \gamma_4 y_{31} + \gamma_5 y_{23} & \gamma_4 x_{13} + \gamma_5 x_{32} & \sigma_9 & \beta_9 y_{31} + \gamma_9 y_{23} & \beta_9 x_{13} + \gamma_9 x_{32} \\ \sigma_8 & \gamma_7 y_{31} + \gamma_8 y_{23} & \gamma_7 x_{13} + \gamma_8 x_{32} & \sigma_6 & \beta_6 y_{31} + \gamma_6 y_{23} & \beta_6 x_{13} + \gamma_6 x_{32} \\ \sigma_2 & \gamma_1 y_{31} + \gamma_2 y_{23} & \gamma_1 x_{13} + \gamma_2 x_{32} & \sigma_3 & \beta_3 y_{31} + \gamma_3 y_{23} & \beta_3 x_{13} + \gamma_3 x_{32} \\ \sigma_4 & \beta_4 y_{31} + \beta_5 y_{23} & \beta_4 x_{13} + \beta_5 x_{32} \\ \sigma_7 & \beta_7 y_{31} + \beta_8 y_{23} & \beta_7 x_{13} + \beta_8 x_{32} \\ \sigma_1 & \beta_1 y_{31} + \beta_2 y_{23} & \beta_1 x_{13} + \beta_2 x_{32} \end{bmatrix} \quad (21)$$

$$\begin{aligned} \beta_1 &= \beta_{10} + \beta_{11}\lambda_1 + \beta_{12}\lambda_2 + \beta_{13}\lambda_3, & \beta_2 &= \beta_{20} + \beta_{21}\lambda_1 + \beta_{22}\lambda_2 + \beta_{23}\lambda_3, & \beta_3 &= \beta_{30} + \beta_{31}\lambda_1 + \beta_{32}\lambda_2 + \beta_{33}\lambda_3, \\ \beta_4 &= \beta_{40} + \beta_{41}\lambda_1 + \beta_{42}\lambda_2 + \beta_{43}\lambda_3, & \beta_5 &= \beta_{50} + \beta_{51}\lambda_1 + \beta_{52}\lambda_2 + \beta_{53}\lambda_3, & \beta_6 &= \beta_{60} + \beta_{61}\lambda_1 + \beta_{62}\lambda_2 + \beta_{63}\lambda_3, \\ \beta_7 &= \beta_{70} + \beta_{71}\lambda_1 + \beta_{72}\lambda_2 + \beta_{73}\lambda_3, & \beta_8 &= \beta_{80} + \beta_{81}\lambda_1 + \beta_{82}\lambda_2 + \beta_{83}\lambda_3, & \beta_9 &= \beta_{90} + \beta_{91}\lambda_1 + \beta_{92}\lambda_2 + \beta_{93}\lambda_3, \\ \gamma_1 &= \beta_1 + \beta_3, & \gamma_2 &= \beta_3, & \gamma_3 &= \beta_2 + \beta_3, & \gamma_4 &= \beta_4 + \beta_9, & \gamma_5 &= \beta_9, & \gamma_6 &= \beta_6 + \beta_8, \\ \gamma_7 &= \beta_6 + \beta_7, & \gamma_8 &= \beta_6, & \gamma_9 &= \beta_5 + \beta_9, & \sigma_1 &= 2\gamma_3 - 2\gamma_1, & \sigma_2 &= 2\gamma_1, & \sigma_3 &= -2\gamma_3, \\ \sigma_4 &= 2\gamma_9 - 2\gamma_4, & \sigma_5 &= 2\gamma_4, & \sigma_6 &= -2\gamma_6, & \sigma_7 &= 2\gamma_6 - 2\gamma_7, & \sigma_8 &= 2\gamma_7, & \sigma_9 &= -2\gamma_9 \end{aligned}$$

$$\mathbf{B}_{\chi 5} = \begin{bmatrix} \sigma_1 & \beta_1 y_{12} + \beta_2 y_{31} & \beta_1 x_{21} + \beta_2 x_{13} & \sigma_2 & \gamma_1 y_{12} + \gamma_2 y_{31} & \gamma_1 x_{21} + \gamma_2 x_{13} \\ \sigma_4 & \beta_4 y_{12} + \beta_5 y_{31} & \beta_4 x_{21} + \beta_5 x_{13} & \sigma_5 & \gamma_4 y_{12} + \gamma_5 y_{31} & \gamma_4 x_{21} + \gamma_5 x_{13} \\ \sigma_7 & \beta_7 y_{12} + \beta_8 y_{31} & \beta_7 x_{21} + \beta_8 x_{13} & \sigma_8 & \gamma_7 y_{12} + \gamma_8 y_{31} & \gamma_7 x_{21} + \gamma_8 x_{13} \\ \sigma_3 & \beta_3 y_{12} + \gamma_3 y_{31} & \beta_3 x_{21} + \gamma_3 x_{13} \\ \sigma_9 & \beta_9 y_{12} + \gamma_9 y_{31} & \beta_9 x_{21} + \gamma_9 x_{13} \\ \sigma_6 & \beta_6 y_{12} + \gamma_6 y_{31} & \beta_6 x_{21} + \gamma_6 x_{13} \end{bmatrix} \quad (22)$$

$$\begin{aligned} \beta_1 &= \beta_{10} + \beta_{11}\lambda_2 + \beta_{12}\lambda_3 + \beta_{13}\lambda_1, & \beta_2 &= \beta_{20} + \beta_{21}\lambda_2 + \beta_{22}\lambda_3 + \beta_{23}\lambda_1, & \beta_3 &= \beta_{30} + \beta_{31}\lambda_2 + \beta_{32}\lambda_3 + \beta_{33}\lambda_1, \\ \beta_4 &= \beta_{40} + \beta_{41}\lambda_2 + \beta_{42}\lambda_3 + \beta_{43}\lambda_1, & \beta_5 &= \beta_{50} + \beta_{51}\lambda_2 + \beta_{52}\lambda_3 + \beta_{53}\lambda_1, & \beta_6 &= \beta_{60} + \beta_{61}\lambda_2 + \beta_{62}\lambda_3 + \beta_{63}\lambda_1, \\ \beta_7 &= \beta_{70} + \beta_{71}\lambda_2 + \beta_{72}\lambda_3 + \beta_{73}\lambda_1, & \beta_8 &= \beta_{80} + \beta_{81}\lambda_2 + \beta_{82}\lambda_3 + \beta_{83}\lambda_1, & \beta_9 &= \beta_{90} + \beta_{91}\lambda_2 + \beta_{92}\lambda_3 + \beta_{93}\lambda_1, \end{aligned}$$

$$\begin{aligned}
\gamma_1 &= \beta_1 + \beta_3, & \gamma_2 &= \beta_3, & \gamma_3 &= \beta_2 + \beta_3, & \gamma_4 &= \beta_4 + \beta_9, & \gamma_5 &= \beta_9, & \gamma_6 &= \beta_6 + \beta_8, \\
\gamma_7 &= \beta_6 + \beta_7, & \gamma_8 &= \beta_6, & \gamma_9 &= \beta_5 + \beta_9, & \sigma_1 &= 2\gamma_3 - 2\gamma_1, & \sigma_2 &= 2\gamma_1, & \sigma_3 &= -2\gamma_3 \\
\sigma_4 &= 2\gamma_9 - 2\gamma_4, & \sigma_5 &= 2\gamma_4, & \sigma_6 &= -2\gamma_6, & \sigma_7 &= 2\gamma_6 - 2\gamma_7, & \sigma_8 &= 2\gamma_7, & \sigma_9 &= -2\gamma_9
\end{aligned}$$

$$\mathbf{B}_{\gamma_6} = \begin{bmatrix} \sigma_6 & \beta_6\gamma_{23} + \gamma_6\gamma_{12} & \beta_6x_{32} + \gamma_6x_{21} & \sigma_7 & \beta_7\gamma_{23} + \beta_8\gamma_{12} & \beta_7x_{32} + \beta_8x_{21} \\ \sigma_3 & \beta_3\gamma_{23} + \gamma_3\gamma_{12} & \beta_3x_{32} + \gamma_3x_{21} & \sigma_1 & \beta_1\gamma_{23} + \beta_2\gamma_{12} & \beta_1x_{32} + \beta_2x_{21} \\ \sigma_9 & \beta_9\gamma_{23} + \gamma_9\gamma_{12} & \beta_9x_{32} + \gamma_9x_{21} & \sigma_4 & \beta_4\gamma_{23} + \beta_5\gamma_{12} & \beta_4x_{32} + \beta_5x_{21} \\ \sigma_8 & \gamma_7\gamma_{23} + \gamma_8\gamma_{12} & \gamma_7x_{32} + \gamma_8x_{21} \\ \sigma_2 & \gamma_1\gamma_{23} + \gamma_2\gamma_{12} & \gamma_1x_{32} + \gamma_2x_{21} \\ \sigma_5 & \gamma_4\gamma_{23} + \gamma_5\gamma_{12} & \gamma_4x_{32} + \gamma_5x_{21} \end{bmatrix} \quad (23)$$

Equations (19) through (23) complete the definition of the KPT-1-36 template.

References

Argyris J, Tenek L, Olofsson L (1997) TRIC: a simple but sophisticated 3-node triangular element based on 6 rigid body and 12 straining modes for fast computational simulations of arbitrary isotropic and laminate composite shells. *Comput. Meth. Appl. Mech. Eng.* 145:11-86

Batoz JL, Bathe K-J and Ho LW (1980) A study of three-node triangular plate bending elements. *Int. J. Num. Meth. Eng.* 15:1771-1812

Batoz JL (1982) An explicit formulation for an efficient triangular plate-bending element. *Int. J. Num. Meth. Eng.* 18:1077-1089

Bazeley GP, Cheung YK, Irons BM, Zienkiewicz OC (1966) Triangular elements in plate bending – conforming and non-conforming solutions. In: *Proceedings 1st Conference on Matrix Methods in Structural Mechanics*, AFFDL-TR-66-80. Air Force Institute of Technology, Dayton, Ohio, pp. 547-584

Bergan PG, Felippa CA (1985) A triangular membrane element with rotational degrees of freedom. *Comput. Meth. Appl. Mech. Eng.* 50:25-69

Bergan PG, Hansen L (1975) A new approach for deriving ‘good’ finite elements. MAFELAP II Conference, Brunel University, 1975. In: *The Mathematics of Finite Elements and Applications – Volume II*, ed. by J. R. Whiteman, Academic Press, London, pp. 483-497

Bergan PG (1980) Finite elements based on energy orthogonal functions. *Int. J. Num. Meth. Eng.* 15:1141-1555

Bergan PG, Nygård MK (1984) Finite elements with increased freedom in choosing shape functions. *Int. J. Num. Meth. Eng.* 20:643-664

Brito Castro FJ, Militello C, Felippa CA (1997) Parametrized variational principles in dynamics applied to the optimization of dynamic models of plates. *Comput. Mech.* 20:285-294

Clough RW, Tocher JL (1966) Finite element stiffness matrices for the analysis of plate bending, In: *Proceedings 1st Conference on Matrix Methods in Structural Mechanics*, AFFDL-TR-66-80, Air Force Institute of Technology, Dayton, Ohio, pp. 515-547

Felippa CA, Bergan PG (1987) A triangular plate bending element based on an energy-orthogonal free formulation. *Comput. Meth. Appl. Mech. Eng.* 61:129-160

Felippa CA, Militello C (1989) Developments in variational methods for high performance plate and shell elements. In: *Analytical and Computational Models for Shells*, CED Vol. 3, ed. by A.K. Noor, T. Belytschko and J.C. Simo, The American Society of Mechanical Engineers. ASME, New York, pp. 191-216

Felippa CA (1994) A survey of parametrized variational principles and applications to computational mechanics. *Comput. Meth. Appl. Mech. Eng.* 113:109-139

Felippa CA, Haugen B, Militello C (1995) From the individual element test to finite element templates: evolution of the patch test. *Int. J. Numer. Meth. Eng.* 38:199-239

Felippa CA (1996) Recent developments in parametrized variational principles for mechanics. *Comput. Mech.* 18:159-174

Felippa CA, Militello C (1998) Optimal 3-node Kirchhoff plate bending triangles. *Proceedings Fourth World Congress in Computational Mechanics*, Buenos Aires, Argentina, June 28-July 1, 1998

Hansen L, Bergan PG, Syversten TJ (1979) Stiffness derivation based on element convergence requirements, MAFELAP III Conference, Brunel University, 1978. In: *The Mathematics of Finite Elements and Applications – Volume III*, ed. by J.R. Whiteman. Academic Press, London, pp. 83-96

Militello C, Felippa CA (1991) The first ANDES elements: 9-DOF plate bending triangles, *Comput. Meth. Appl. Mech. Eng.* 93:217-246

Nygård MK (1986) The free formulation for nonlinear finite elements with applications to shells. Ph.D. Dissertation. Division of Structural Mechanics, NTH, Trondheim, Norway

Park KC, Stanley GM (1986) A curved C^0 shell element based on assumed natural-coordinate strains. *J. Appl. Mech.* 53:278-290

Stricklin J, Haisler W, Tisdale P, Gunderson R (1969) A rapidly converging triangular plate bending element. *AIAA J.* 7:180-181